Myt1 inhibition of Cyclin A/Cdk1 is essential for fusome integrity and premeiotic centriole engagement in *Drosophila* spermatocytes

Ramya Varadarajan[a], Joseph Ayeni[a], Zhigang Jin[b], Ellen Homola[a], and Shelagh D. Campbell[a,*]
[a]Department of Biological Sciences and [b]Cross Cancer Institute, University of Alberta, Edmonton, AB T6G 2E9, Canada

ABSTRACT **Regulation of cell cycle arrest in premeiotic G2 phase coordinates germ cell maturation and meiotic cell division with hormonal and developmental signals by mechanisms that control Cyclin B synthesis and inhibitory phosphorylation of the M-phase kinase, Cdk1. In this study, we investigated how inhibitory phosphorylation of Cdk1 by Myt1 kinase regulates premeiotic G2 phase of *Drosophila* male meiosis. Immature spermatocytes lacking Myt1 activity exhibit two distinct defects: disrupted intercellular bridges (fusomes) and premature centriole disengagement. As a result, the *myt1* mutant spermatocytes enter meiosis with multipolar spindles. These *myt1* defects can be suppressed by depletion of Cyclin A activity or ectopic expression of Wee1 (a partially redundant Cdk1 inhibitory kinase) and phenocopied by expression of a Cdk1F mutant defective for inhibitory phosphorylation. We therefore conclude that Myt1 inhibition of Cyclin A/Cdk1 is essential for normal fusome behavior and centriole engagement during premeiotic G2 arrest of *Drosophila* male meiosis. The novel meiotic functions we discovered for Myt1 kinase are spatially and temporally distinct from previously described functions of Myt1 as an inhibitor of Cyclin B/Cdk1 to regulate G2/MI timing.**

Monitoring Editor
Yukiko Yamashita
University of Michigan

Received: Feb 16, 2016
Revised: May 2, 2016
Accepted: May 5, 2016

INTRODUCTION

Opposing Cdk1 inhibitory kinases and Cdc25 phosphatases regulate the activity of Cyclin B/Cdk1 to control the timing of entry into M phase. There are two types of Cdk1 inhibitory kinases: Wee1 nuclear kinases, which exist in all eukaryotic organisms, and Myt1 kinases, which are found only in metazoans and localize to the endoplasmic reticulum (ER) and Golgi membranes (Kornbluth *et al.*, 1994; Mueller *et al.*, 1995; Liu *et al.*, 1997). Studies of oogenesis in *Xenopus laevis*, *Caenorhabditis elegans*, and *Asterina pectinifera* show that Myt1 inhibition of Cyclin B/Cdk1 regulates premeiotic G2-phase arrest (Karaiskou *et al.*, 2004; Inoue and Sagata, 2005; Burrows *et al.*, 2006; Gaffre *et al.*, 2011; Kishimoto, 2011). Therefore inhibition of Myt1 is required for oocyte maturation (Palmer *et al.*, 1998; Ruiz *et al.*, 2010; Gaffre *et al.*, 2011). Myt1 overexpression can also prolong G2 phase in mitotically proliferating mammalian cells (Liu *et al.*, 1999; Wells *et al.*, 1999) and *Drosophila* eye imaginal disks (Price *et al.*, 2002).

Previous studies also showed that Myt1 inhibition of Cyclin B/Cdk1 influences Golgi and ER membrane dynamics. Knockdown of Myt1 by small interfering RNA affects G2/M-linked Golgi fragmentation and can alleviate delays in mitotic entry due to mitogen-activated kinase kinase inhibition in mammalian cells (Villeneuve *et al.*, 2013), and a study using a similar approach found that Myt1 regulation of Cdk1 activity during telophase was essential for Golgi and ER assembly during mitotic exit (Nakajima *et al.*, 2008; Villeneuve *et al.*, 2013). Golgi/ER dynamics was also affected by RNA interference depletion in *Drosophila* cells (Cornwell *et al.*, 2002). Cell cycle regulation by Myt1 inhibition of Cyclin B/Cdk1 therefore appears to be important both for maintenance of G2-phase arrest and to coordinate endomembrane dynamics with M phase.

Genetic studies of *Drosophila melanogaster* loss-of-function *myt1* mutants revealed mitotic proliferation defects during imaginal

This article was published online ahead of print in MBoC in Press (http://www.molbiolcell.org/cgi/doi/10.1091/mbc.E16-02-0104) on May 11, 2016.

*Address correspondence to: Shelagh D. Campbell (shelagh.campbell@ualberta.ca).

Abbreviations used: BrdU, bromo-deoxyuridine; Cdk1, Cyclin-dependent kinase 1; ER, endoplasmic reticulum; Plk1, Polo-related kinase 1.

disk development as well as in gametogenesis in both sexes (Jin *et al.*, 2005). These mutants are viable because of functional redundancy with Wee1 (Jin *et al.*, 2008; Kao *et al.*, 2015) and are male-sterile but female-fertile presumably because *Drosophila* oocytes arrest not in premeiotic G2 phase but in metaphase I (McKim *et al.*, 1993), whereas spermatocytes undergo a developmentally regulated premeiotic arrest in G2 phase before initiating meiosis I (Fuller, 1998). These findings suggest that Myt1 regulates premeiotic G2-phase arrest of *Drosophila* male meiosis.

Drosophila male germ cells undergo four transit-amplifying mitotic divisions with incomplete cytokinesis, producing 16-cell cysts that are interconnected by organelles called fusomes derived from the ER (Hime *et al.*, 1996; Eikenes *et al.*, 2013). After differentiating, spermatocytes undergo premeiotic S phase and then arrest in G2 phase for ~90 h before initiating meiosis I. The timing of the G2/MI transition is triggered by unknown developmental cues regulating transcriptional and translational mechanisms that restrict synthesis of Cyclin B and other essential meiotic regulators to late G2 phase (White-Cooper *et al.*, 1998; Baker and Fuller, 2007; Baker *et al.*, 2015; Franklin-Dumont *et al.*, 2007). One of these essential regulators is the meiotic $Cdc25^{Twe}$ phosphatase (Twine), which removes inhibitory phosphorylation from Cyclin B/Cdk1, driving the G2/MI transition (Alphey *et al.*, 1992; Courtot *et al.*, 1992; White-Cooper *et al.*, 1993; Sigrist *et al.*, 1995). Unlike Cyclin B, whose expression is repressed until late G2 phase, Cyclin A is expressed throughout premeiotic G2 phase, and the protein accumulates on intercellular fusome bridges (Lilly *et al.*, 2000). Inhibition of Cyclin A/Cdk1 by Rux is essential for normal cell cycle exit from meiosis II (Gonczy *et al.*, 1994); however, specific functions for Cyclin A/Cdk1 during male meiosis have not yet been reported.

In this study, we sought to understand the essential functions of Myt1 kinase during *Drosophila* male meiosis by phenotypic analysis of male-sterile *myt1* mutants. We discovered that Myt1 inhibition of Cdk1/Cyclin A is essential for fusome integrity and centriole engagement during the prolonged premeiotic G2-phase arrest. These meiotic functions of Myt1 are mechanistically distinct from previously described roles in regulation of G2-phase arrest by inhibition of Cdk1/Cyclin B.

RESULTS

Timing of G2/MI appears relatively normal in *myt1* mutant spermatocytes

In many organisms, Myt1 inhibition of Cyclin B/Cdk1 is required for premeiotic G2-phase arrest during female meiosis (Palmer *et al.*, 1998; Nakajo *et al.*, 2000; Burrows *et al.*, 2006; Oh *et al.*, 2010; Gaffre *et al.*, 2011). To investigate whether Myt1 plays a similar role during *Drosophila* male meiosis, we examined loss-of-function *myt1* mutants (Jin *et al.*, 2005) to assess the timing of premeiotic G2-phase arrest. For this experiment, we briefly feed adult males with 5-bromo-2-deoxyuridine (BrdU) to label postmitotic 16-cell spermatocyte cysts (see *Materials and Methods*). To detect cysts that incorporated BrdU during premeiotic S phase, testes were dissected, fixed, and immunolabeled at timed intervals using established cytological criteria for staging spermatocytes, as shown in Figure 1A (Cenci *et al.*, 1994). Representative examples of *myt1/+* control cysts fixed at 24, 72, and 93 h post-BrdU pulse are shown in Figure 1B, corresponding to polar (S1–S2), apolar (S3–S4), and mature (S5–S6) stages of spermatocyte maturation. At the 93-h postlabeling time point, the stage S5 control spermatocytes had intact nucleoli and three major chromosome compartments in the nucleus; by stage S6–prophase I, the nucleoli had disassembled and the chromosomes condensed, signifying that the G2/MI transition had occurred.

As previously reported (Jin *et al.*, 2005), we observed examples of BrdU-labeled *myt1* mutant cysts undergoing ectopic gonial mitotic divisions at the earliest postlabel time points (24 h postchase), which we did not further analyze (unpublished data). To compare the relative timing of premeiotic G2 phase in different genotypes, we pooled data for the BrdU-labeled cysts from testes fixed at 93 ± 2 h postchase labeled spermatocytes as a point of reference for late G2 phase. In data from four independent experiments shown in Figure 1C, 93% of the labeled *myt1/+* control spermatocytes (n = 238) had intact nucleoli like those shown in Supplemental Figure S1B (arrowheads) and stage S5 DNA morphology (Figure 1B and Supplemental Figure S1C). In *myt1* mutants, only 64% of the labeled spermatocytes (n = 291) had intact nucleoli, whereas the remaining 36% of the *myt1* mutant spermatocytes had nucleoli that appeared fragmented, even though the chromatin had not undergone the condensation characteristic of stage S6–prophase I (Supplemental Figure S1E, cells marked by asterisk and arrowhead). The BrdU-labeled chromosomes of *myt1* mutant spermatocytes also appeared less condensed than similarly staged controls (compare Supplemental Figure S1, C and F). These variations in nucleolar morphology could even be observed within a single *myt1* mutant cyst (compare nuclei marked by asterisks or arrowheads, Supplemental Figure S1, E and F). In parallel experiments analyzing zygotic *wee1* mutants lacking the partially redundant Cdk1 inhibitory kinase Wee1, 96% of the BrdU-labeled spermatocytes had intact nucleoli, indistinguishable from the controls (data from two independent experiments; n = 121; see also Supplemental Figure S1, G–I).

By 100 h after the BrdU pulse, *myt1/+* control cysts with ~32 cells were observed (Supplemental Figure S1J; two cysts), indicating that meiosis I was completed between 93 and 100 h under these conditions. By 111 h, cysts with ~64 cells were observed (Supplemental Figure S1K; two cysts), indicating that the meiosis II divisions were completed. BrdU-labeled *myt1* mutant cysts fixed at these time points showed similar results (Supplemental Figure S1, J and K), from which we conclude that the timing of meiotic events was relatively normal in the *myt1* mutants.

To examine G2/MI progression in more detail, we compared fixed, cytologically staged *myt1/+* and *myt1* mutant spermatocytes by immunolabeling for lamin DmO and phospho (S10)-histone H3 (PH3) to characterize the relationship between nuclear envelope breakdown and meiotic chromosome condensation. In *myt1/+* control spermatocytes, the nuclear lamina was intact until late prophase I but had partially disassembled by the time PH3 labeling appeared, and the chromosomes coalesced during prometaphase (Figure 1D). These features of G2/MI appeared similarly coordinated in the *myt1* spermatocytes (Figure 1D). We also examined Cyclin A translocation into the nucleus at the G2/MI transition (Gonczy *et al.*, 1994; Franklin-Dumont *et al.*, 2007). In stage S6 control spermatocytes, Cyclin A was primarily cytoplasmic and enriched at the fusomes (arrow, Figure 1E). By prometaphase I, Cyclin A could also be observed in the nucleus, signifying G2/M. We also observed that Cyclin A was primarily cytoplasmic in stage S6 and entered the nucleus at prometaphase I in *myt1* mutant spermatocytes; however, fusome labeling was undetectable (Figure 1E). The timing of Cyclin A translocation into the nucleus therefore appeared normal in *myt1* mutant spermatocytes. We therefore concluded that the timing of premeiotic G2 phase arrest did not depend on Myt1 activity, but the observed nucleolar fragmentation, chromosome condensation defects, and absence of Cyclin A fusome enrichment in *myt1* mutants indicated that certain meiotic processes were sensitive to loss of Myt1.

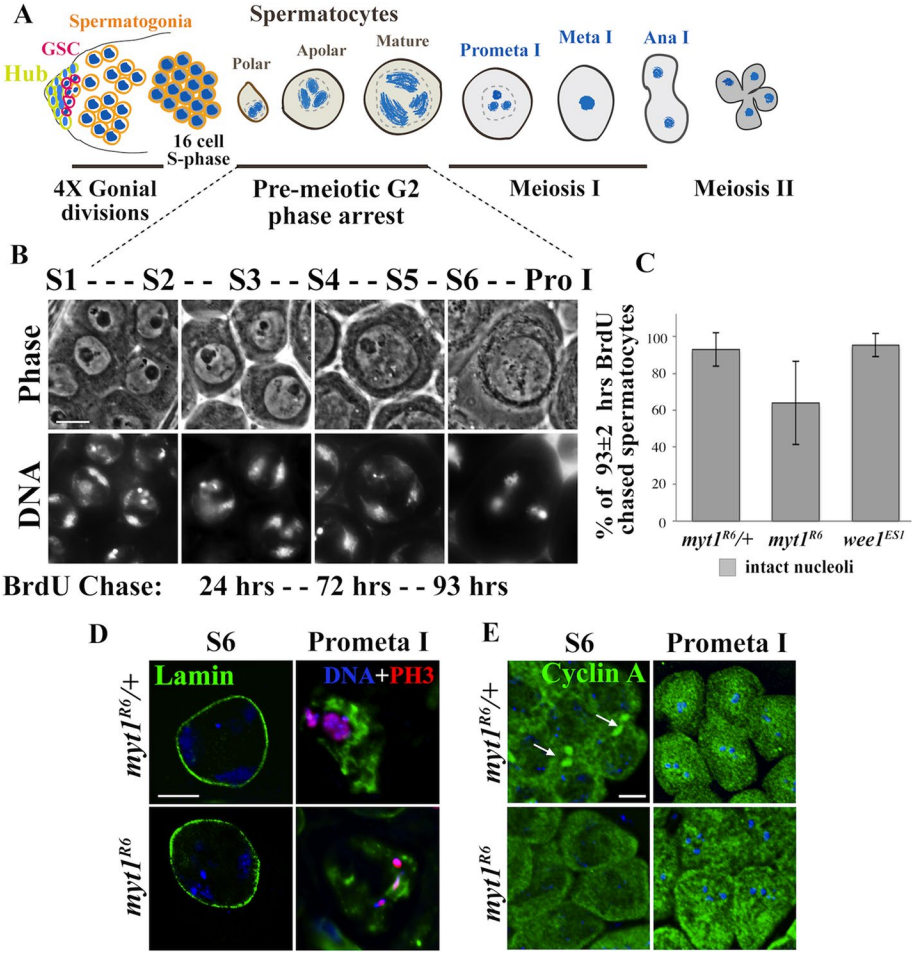

FIGURE 1: Temporal coordination of G2/MI is relatively normal in *myt1* spermatocytes. (A) Stages of *Drosophila* spermatocyte maturation, showing characteristic chromosome morphology features (Cenci *et al.*, 1994). (B) Chromosome and cellular morphology of live DNA-labeled stage S1–S6 spermatocytes examined by phase contrast microscopy. Numbers (underneath) refer to time after BrdU labeling (24, 72, and 93 h postchase) corresponding to early (S1–S2), mid (S3–S4), and late (S5–S6) stages of premeiotic G2 phase. Scale bar, 10 µm. (C) Graph comparing percentages of labeled spermatocytes at 93 ± 2 h post-BrdU with intact nucleoli. Error bar indicates SD of the mean (SM). These data were derived from *n* independent experiments for each genotype: *myt1/+* controls ($n = 4$, SM = 9.05), *myt1* mutants ($n = 4$, SM = 22.5), and *wee1* mutants ($n = 4$, SM = 6.4). The total number of spermatocytes examined for each genotype in these experiments was 238 for *myt1/+*, 291 for *myt1*, and 121 for *wee1*. In *myt1* mutant testes examined at 93 ± 2 h post-BrdU, we observed 64% of spermatocytes with intact nucleoli; the rest had fragmented nucleoli. Student's *t* test was performed to determine whether there were significant differences between the *myt1/+* control and *myt1* data sets. Means of the two genotypes were not significantly different at $p < 0.05$ (*t* value, 1.8898 less than critical value, 2.571). (D) Relationship between meiotic nuclear envelope breakdown and chromosome condensation in *myt1/+* control and *myt1* mutant spermatocytes at the indicated stages of meiosis I by immunolabeling for lamin (DmO; green) and phospho–histone H3 (PH3; red) and DNA labeling. Scale bar, 10 µm. The *myt1/+* and *myt1*-mutant stage S6 spermatocytes both have an intact nuclear lamina, which disassembles by prometaphase I when PH3 labeling is detected. The spermatocytes are not perfectly matched for prometaphase I but were at slightly different stages (Cenci *et al.*, 1994) and were the best PH3-labeled cysts we found for this comparison. (E) Cell cycle–dependent localization of Cyclin A (green) detected by immunolabeling and Hoechst labeling (blue). Cyclin A is detected primarily in the cytoplasm in stage S6 *myt1/+* and *myt1* mutant spermatocytes, but by prometaphase I, it can also be seen in the nucleus. Arrows shown in *myt1/+* mature spermatocytes indicate Cyclin A enrichment at fusomes, which is absent in *myt1* mutants. Scale bar, 16 µm.

Loss of Myt1 activity disrupts ER-derived fusomes specifically at the mitotic–meiotic transition

Previous studies implicated Myt1 inhibition of Cyclin B/Cdk1 activity in the mitotic regulation of Golgi and ER membrane remodeling (Nakajima *et al.*, 2008). Because the timing of premeiotic G2-phase arrest appeared relatively unaffected in the *myt1* spermatocytes, we considered whether defects in endomembrane remodeling or organelle dynamics might underlie the mutant phenotype. As a first test of this idea, we immunolabeled spermatocytes with antibodies to Lava lamp (Lva), a peripheral Golgi protein (Sisson *et al.*, 2000). In both *myt1/+* and *myt1* mutant stage S5–S6 spermatocytes, ring-shaped structures corresponding to Golgi stacks were observed (Supplemental Figure S2A, inset), with no obvious differences in either number or appearance (Supplemental Figure S2B). We quantified these data by counting Lva-labeled Golgi stacks from merged, deconvolved *Z*-stack images and observed similar numbers in the controls (average = 16, $n = 74$, SD = 2.8) and *myt1* mutants (average = 15, $n = 85$, SD = 3.2). Golgi stacks disassemble for the meiotic divisions before reassembling again to organize the acroblast (Belloni *et al.*, 2012; Yasuno *et al.*, 2013). We observed similar Golgi dynamics at these stages in both the controls and the *myt1* mutant spermatocytes (Supplemental Figure S2C). Golgi behavior was therefore unaffected by loss of Myt1.

Next we examined intercellular bridges with conserved roles in germ cell development (Greenbaum *et al.*, 2011), called fusomes in *Drosophila*. These membrane-rich, germline-specific organelles derived from the ER are essential for both male and female gametogenesis (Lin *et al.*, 1994; Lin and Spradling, 1995; de Cuevas *et al.*, 1997; McKearin, 1997). We examined the fusomes by immunolabeling the Adducin-related protein Hts (Yue *et al.*, 1992; Zaccai and Lipshitz, 1996). Because fusomes are present throughout male germline development, we also colabeled a nucleolar protein called Spermatocyte arrest (Sa), enabling us to distinguish between the mitotically proliferating spermatogonial cysts and cysts of G2 phase–arrested spermatocytes (Chen *et al.*, 2005). In *myt1/+* controls, Hts-labeled fusomes were observed connecting the cells in both spermatogonial and spermatocyte cysts (Figure 2A). Although the spermatogonial fusomes appeared normal in *myt1* mutant cysts, Hts labeling was almost undetectable in spermatocyte cysts (Figure 2, A, asterisk, B, and C) from as early as stages S1–S2 (Supplemental Figure S3, A and B). Immunolabeling for another fusome protein (α-Spectrin) also revealed fusome defects that specifically affected *myt1* mutant spermatocytes (unpublished data). Loss of Myt1 activity therefore compromised the integrity of fusomes specifically in the premeiotic G2 phase–arrested spermatocytes.

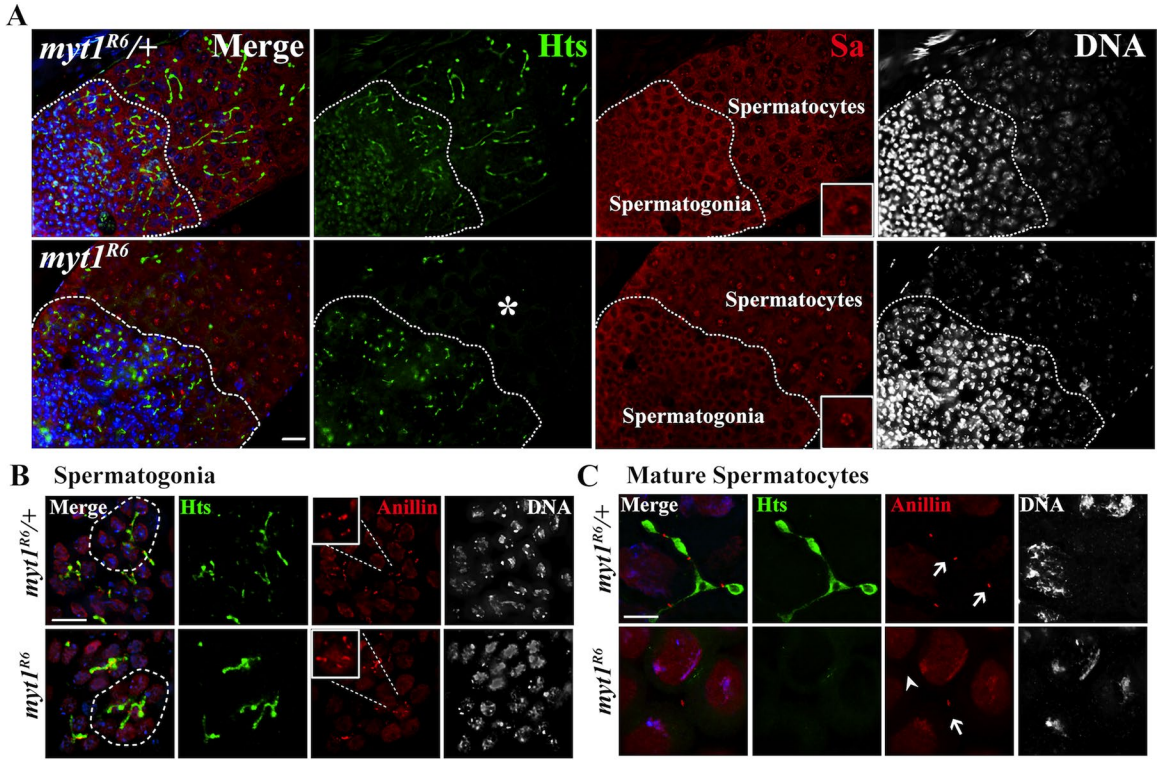

FIGURE 2: Fusome abnormalities in *myt1* mutant spermatocytes. (A) Whole-mount testes colabeled for Hts (fusomes, green) and spermatocyte arrest (Sa, red) and DNA (blue). The pronounced nucleolar localization of Sa (inset) was used as a marker for premeiotic spermatocytes. Hts-labeled fusomes appear normal in both control and *myt1* mutant spermatogonial cysts close to the tip of the testes. Hts labeling of fusomes is undetectable in *myt1* mutant spermatocytes (asterisks) compared with controls. Scale bar, 16 μm. (B, C) Squashed germ cells are colabeled for Hts (fusomes, green), anillin (ring canals, red), and DNA (blue). (B) Eight-cell spermatogonial cysts (circled) showing *myt1/+* control and *myt1* mutant cysts with normal fusomes and ring canals. The insets highlight groups of ring canals from the same cyst. (C) Sixteen-cell *myt1/+* control spermatocytes showing fusomes passing through ring canals (arrows). In *myt1* spermatocytes, the ring canals were harder to detect (arrowheads), and the fusomes were absent. Scale bar, 10 μm.

Fusomes pass through ring canals remaining after incomplete cytokinesis (Hime *et al.*, 1996). To examine the relationship between ring canals and fusomes, we colabeled for Hts and Anillin, a protein that localizes to ring canals (Field and Alberts, 1995), and show representative images of control spermatogonia (Figure 2B, inset) and spermatocyte cysts (Figure 2C, arrows). Although the ring canals appeared normal in *myt1* spermatogonial cysts (Figure 2B, inset), they appeared abnormal and were difficult to detect in mutant cysts (Figure 2C, arrowhead). To examine these intercellular bridges at higher resolution, we analyzed thin sections by transmission electron microscopy. To compare the control and *myt1* mutant spermatocytes, we focused on images in which at least two cells connected by ring canals were clearly seen in more than one section (Figure 3). In *myt1/+* controls (16 pairs of spermatocytes), fusomes (F) appeared as smooth structures interconnecting adjacent spermatocytes that were bordered by two dark parallel lines representing the ring canals in cross section (Figure 3, A and B, arrows). Fusomes and ring canals could also be detected in *myt1* mutant spermatocytes (19 pairs of spermatocytes), but they appeared distorted and narrower than the controls (Figure 3, C–F).

To determine whether these fusome defects were specifically due to loss of Myt1 activity, we created inducible Myt1 transgenes that could be used for rescue experiments (*Materials and Methods*). We initially characterized these Myt1 reporters by Western blot analysis of testes extracts and green fluorescent protein (GFP) fluorescence. Our results showed that the reporters were catalytically active with respect to inhibitory phosphorylation of endogenous Cdk1 in vivo, and the transgenic proteins localized to the ER and Golgi during male meiosis, as expected (Supplemental Figure S4). Examination of intact cysts also showed that early *bam*-driven meiotic expression of enhanced GFP (EGFP)–Myt1 fully rescued *myt1*-mutant fusome defects (Supplemental Figure S5) and restored male fertility (Table 1). Later *topi-Gal4* driven expression of EGFP-Myt1 in stage S5–S6 spermatocytes (Raychaudhuri *et al.*, 2012), however, only partially rescued these defects (Supplemental Figure S5 and Table 1). To quantify the rescue of mutant fusome defects, we counted intact stage S1–S6 cysts with normal or partial fusomes. We observed that *bam*-driven rescue of *myt1* mutants resulted in 100% normal fusomes (28 intact cysts), whereas *topi*-driven rescue resulted in 0% normal, 94% partial, and 6% no rescue (31 intact cysts). Myt1 activity is therefore essential for the integrity of the ER-derived fusomes during premeiotic G2-phase arrest.

Loss of Myt1 activity results in premature centriole disengagement in immature spermatocytes

Previous studies suggested that *myt1* mutant spermatids were aneuploid (Jin *et al.*, 2005). Because defects in centrosomes and meiotic spindle behavior can cause aneuploidy (Vitre and Cleveland, 2012) and centrosome defects were previously associated with disrupted fusomes during *Drosophila* male meiosis (Wilson, 2005), we

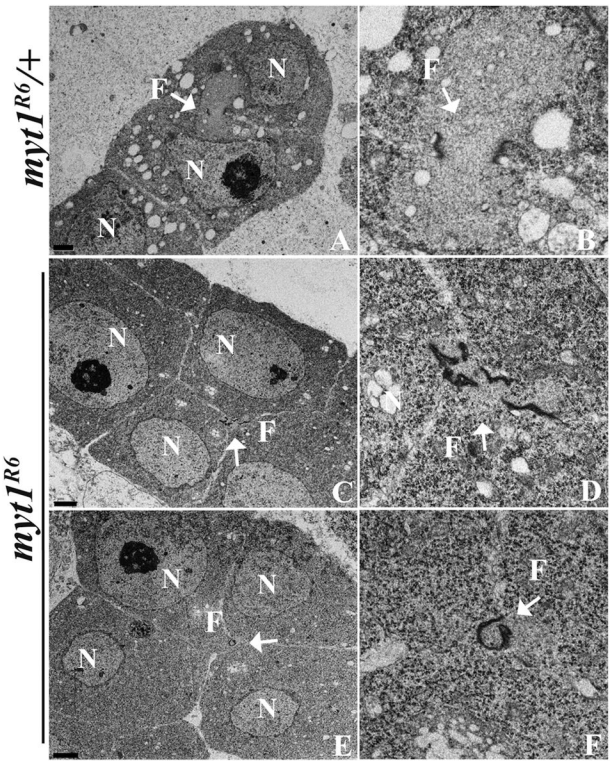

FIGURE 3: Fusomes are disrupted in *myt1* mutant spermatocytes. Thin sections of spermatocytes analyzed by transmission electron microscopy, annotated for nucleus (N) and fusome (F). (A, B) *myt1/+* control spermatocytes are interconnected by smooth cytoplasmic bridges bounded by two dark, parallel lines showing the fusomes (F; arrow) and ring canals, respectively (16 pairs of spermatocytes examined). (C–F) The *myt1* mutant spermatocytes had abnormal cytoplasmic bridges and ring canals (19 pairs of spermatocytes examined), including disrupted (seven of 19; C, D) and constricted (four of 19; E, F) fusomes, respectively. Scale bar, 2 µm (A, C, E), 1 µm (B, D, F).

examined how loss of Myt1 activity affected centrosomes and meiotic spindles. In *myt1/+* control spermatocytes immunolabeled for centrosomin (Cnn) and β-tubulin (Li *et al.*, 1998), we observed bipolar meiotic spindles (Figure 4A). In contrast, *myt1* mutant spermatocytes exhibited multipolar meiotic spindles, usually with four distinct Cnn-labeled foci. These defects could be rescued by GFP-tagged-Myt1 expression in mid G2 phase under control of the β2-tubulin (*tv3*) promoter (Figure 4A). Loss of Myt1 activity therefore results in multipolar meiotic spindle defects expected to cause aneuploidy that would contribute to *myt1* mutant male sterility. In spite of the high penetrance of these centrosome defects, however, most early postmeiotic *myt1* cysts appeared relatively normal (Figure 4B and Supplemental Figure S1K).

Antibodies recognizing a phosphorylated form of Aurora A (AurA-T288p) that labels centrioles can be used for visualizing centrosome dynamics (Eyers *et al.*, 2003; Tsai *et al.*, 2003). Using these antibodies to examine premeiotic centrosome behavior, we observed that the *myt1/+* stage S3–S4 control spermatocytes each had a pair of closely associated centrosomes; by stages S5–S6, each centrosome consisted of a pair of elongated centrioles with a characteristic V-shaped structure (Figure 4B). By late anaphase I, centriole disengagement could be observed (Figure 4B, asterisks), resulting in each spermatid receiving one centriole after completion of meiosis II. In contrast, examination of *myt1* mutant spermatocytes revealed distinct AurA-T288p–labeled foci as early as stages S3–S4 (Figure 4B, asterisk), ~2 d before centriole disengagement would normally occur. By stages S5–S6, there were usually four (but never more) elongated AurA-T288p–labeled foci in the *myt1* mutant spermatocytes, and, not surprisingly, the *myt1* mutant spermatids had variable numbers of centrioles, presumably indicating segregation defects during the meiotic cell divisions (Figure 4A). We quantified similar results using another centrosome marker (monoclonal antibody GTU-88), as shown in Figure 4C. These results therefore demonstrated for the first time that Myt1 activity is essential for normal meiotic centrosome behavior and spindle dynamics.

Polo (PLK1) kinase regulates mitotic centriole disengagement (Wang *et al.*, 2008; Tsou *et al.*, 2009; Cabral *et al.*, 2013; Zitouni *et al.*, 2014), and treatment with a Polo inhibitor can block centriole disengagement in *Drosophila* spermatocytes (Riparbelli *et al.*, 2014). We therefore used RNA interference (RNAi) to examine whether a Polo-dependent centriole disengagement mechanism might be involved in this aspect of the *myt1* mutant phenotype. As a control to test whether transgenic double-strand RNA expression would affect spermatocytes, we first examined *bam*-driven *polo*^{siRNA} alone. When *bam*-driven *polo*^{siRNA} was expressed in *myt1*/+ controls, 82% of late meiosis I–stage spermatocytes (see Figure 4B for comparison) labeled with Aurora A-T288p retained elongated V-shaped centrosomes (Figure 4D; $n = 248$). These results indicated that RNAi depletion of Polo activity blocked centriole disengagement at meiosis I, as expected. When *bam*-driven *polo*^{siRNA} was expressed in *myt1* mutant spermatocytes, we also observed pairs of elongated V-shaped meiotic centrosomes, indicating that Polo depletion was able to rescue the *myt1* mutant premature centriole

Degree of fertility	*myt1*^{R6}/+	*myt1*^{R6}	*bam* > *Myt1*	*topi* > *Myt1*	*bam* > *Wee1*	*Rux*	*CycA*^{siRNA}	*polo*^{siRNA}	*Cdk1WT*	*Cdk1F*	*Cdk1AF*
Fertile	30	0	17	13	29	3*	0	0	23	18	7
Semifertile	0	0	1	2	0	6	0	0	2	6	2
Sterile	0	30	2	5	1	23	25	20	0	8	15
Number of males	30	30	20	20	30	32	25	20	25	32	24

Single males of the indicated genotypes were each crossed with three *yw* virgin females ,and the entire first brood of progeny was counted (<10 d after first eclosion at 25°C). Male fertility was classified according to Gonczy *et al.* (1994) by counting the progeny produced by each male: fertile (100–150 progeny), semifertile (<20 progeny), and sterile (no progeny). In one case (marked by asterisk), the *rux*-expressing males in a *myt1* background were technically fertile with >20 progeny, but each male had <50 progeny, and the progeny were developmentally delayed. All of the genotypes shown in gray highlighting refer to the indicated transgenes expressed in a *myt1*^{R6} mutant background.

TABLE 1: Rescue of *myt1*^{R6} mutant male sterility.

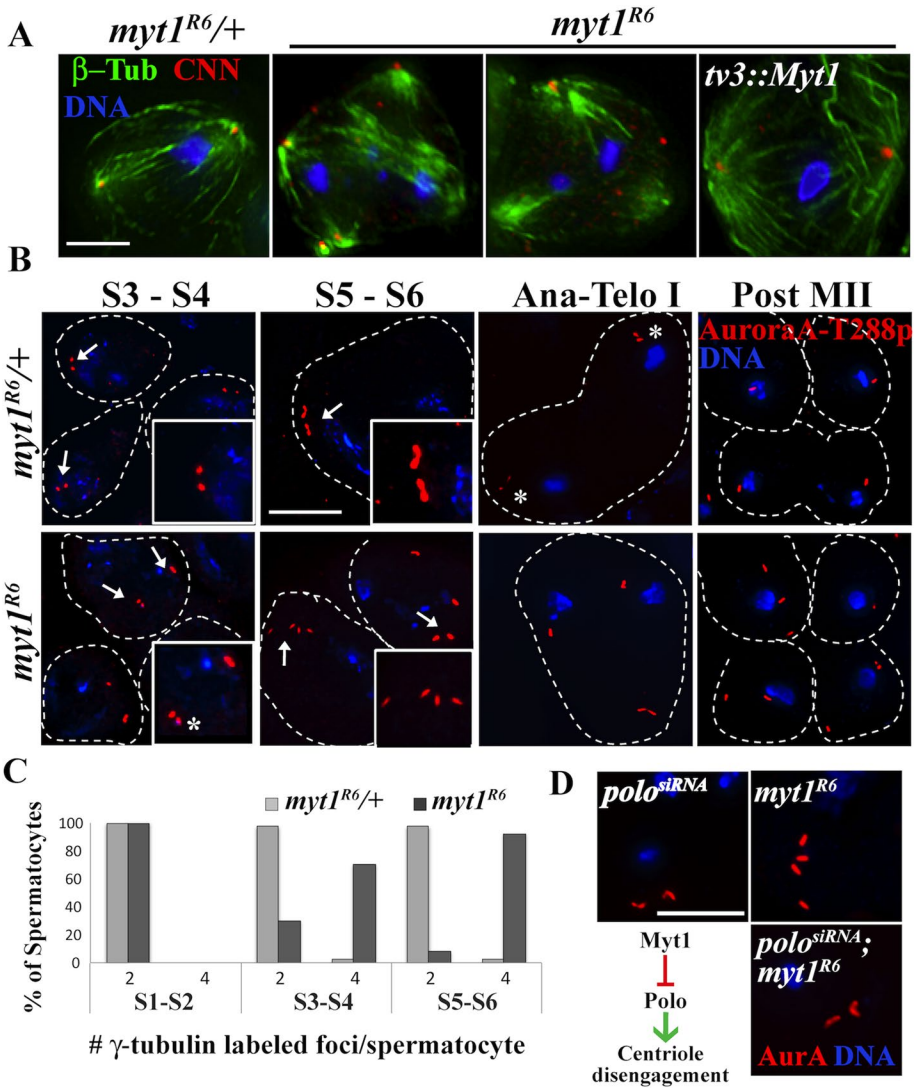

FIGURE 4: *myt1* meiotic spindle defects are due to Polo-mediated premature centriole disengagement. (A) Loss of Myt1 activity causes premature centriole disengagement and multipolar spindles and can be rescued by transgenic GFP-Myt1. Meiotic spindles were immunolabeled for β-tubulin (green) and centrosomin (Cnn, red) and stained for DNA (blue). Cnn labels the pericentriolar matrix (PCM), and the antibodies exhibit some nonspecific background signals. Scale bar, 8 μm. (B) Loss of Myt1 results in premature centriole disengagement. Premeiotic centrosomes were immunolabeled for AuroraA-T288p (red) and DNA (blue). In *myt1/+* controls, stage S3–S4 spermatocytes exhibit two paired AuroraA-T288p foci per cell (arrows), each representing one centrosome. Stage S5–S6 control spermatocytes have elongated, V-shaped centrosomes, each representing a pair of orthogonally engaged centrioles (inset). During anaphase I, the centrioles disengage (asterisks), so that by completion of meiosis II, each daughter cell has one centriole. In the *myt1*-mutant stage S3–S4 spermatocytes, we often observed more than two AuroraA-T288p–labeled foci (asterisks), resembling the disengaged centrioles in anaphase–telophase I controls. In stages S5–S6 *myt1* mutant spermatocytes, four distinct AuroraA-T288p foci were usually seen (arrows) instead of two V-shaped centrosomes. These prematurely disengaged centrioles appeared to be randomly distributed in anaphase I *myt1* mutants, resulting in postmeiotic cells with variable numbers of centrioles. Scale bar, 10 μm. (C) Quantification of *myt1* mutant centrosome defect at different stages of spermatocyte maturation. Graph indicates percentage of spermatocytes with two or four γ-tubulin–labeled foci at early (S1–S2), mid (S3–S4), and late (S5–S6) stages of maturation. At stages S1–S2, both *myt1/+* controls and *myt1* mutants exhibit two labeled foci per cell. By stages S3–S4, 70.2% (191) of *myt1* mutants had more than two foci (see B, inset, asterisks). By stages S5–S6, 92.2% (192) of the *myt1* mutant spermatocytes exhibit four elongated foci per cell. (D) Depletion of Polo kinase by *bam-Gal4>polo*^{siRNA} in a *myt1/+* control blocked centriole disengagement in 82% (248) of mature spermatocytes (stage S5–prometaphase I), resulting in elongated, V-shaped centrosomes. When *bam-Gal4>polo*^{siRNA} was expressed in a *myt1* background, we observed elongated, V-shaped centrosomes in 71% (157) of mature spermatocytes examined, showing that Polo depletion phenotypically rescued the premature centriole disengagement defect. Scale bar, 10 μm. Bottom left, model depicting the relationship between Myt1 and a Polo-mediated centriole disengagement mechanism.

disengagement defect (Figure 4D). To quantify this phenotypic rescue, we analyzed stage S5–to-prometaphase spermatocytes, observing that expression of *bam*-driven *polo*^{siRNA} in a *myt1* mutant background suppressed premature centriole disengagement to 29% (n = 157), whereas in *myt1* mutants alone, 92% of the spermatocytes were disengaged at this stage (Figure 4C; n = 192). Expression of *bam*-driven *polo*^{siRNA} had no effect, however, on the *myt1* mutant fusome defect (unpublished data). These results indicated that the premature centriole disengagement and meiotic spindle defects caused by loss of Myt1 activity were due to aberrant Polo activity and were not an indirect consequence of earlier defects in fusome integrity.

Ectopic expression of Wee1 rescued *myt1* mutant sterility but not fusome defects

To assess how Cdk1 inhibitory phosphorylation affected the *myt1* mutant phenotype, we examined the partially redundant kinase Wee1. Loss-of-function *wee*^{ES1} mutant spermatocytes had normal Hts-labeled fusomes (Supplemental Figure S6A), and *bam*-driven *UAS-Wee1* expression in a *myt1/+* control background also resulted in normal meiotic fusomes (Supplemental Figure S6B). Moreover, expression of *UAS-Wee1* did not rescue the *myt1* mutant fusome defects (Supplemental Figure S6B). We quantified these results by examining stage S1–S6 mutant cysts expressing *UAS-Wee1* and counted 0% cysts with intact fusomes, 12% with partial fusomes, and 88% with disrupted fusomes (n = 28).

In contrast, we observed that *UAS-Wee1* expression rescued the *myt1*-mutant centriole engagement and spindle abnormalities in spermatocytes immunolabeled with Hts and AuroraA-T288p (Supplemental Figure S6C) and also restored male fertility (Table 1). To quantify this effect, we counted stage S5–to-prometaphase *myt1* mutant spermatocytes expressing *UAS-Wee1* and observed almost complete rescue (only 5% with disengaged centrioles; n = 94). These results showing that Wee1 suppressed *myt1* mutant premature centriole disengagement and male sterility without rescuing the fusome defect led us to conclude that Myt1

inhibition of Cdk1 is necessary for regulating centrosome behavior during premeiotic G2 phase.

Expression of Cdk1(Y15F) phenocopies *myt1*-mutant organelle defects

Wee1 and Myt1 can both catalyze inhibitory phosphorylation of Cdk1 on residue Y15, but only Myt1 phosphorylates Cdk1 on residue T14 (Jin *et al.*, 2008). As another method for testing how inhibitory phosphorylation of Cdk1 affected male meiosis, we expressed a transgenic mutant Cdk1(Y15F) that cannot be phosphorylated on Y15. Previous studies with Gal4-inducible Cdk1(Y15F):VFP showed that the expressed protein could form complexes with mitotic cyclins A and B, triggering Cdk1 activation to drive the G2/M transition (Ayeni *et al.*, 2014). We therefore constructed transgenic strains to express Cdk1(WT) and Cdk1(Y15F) reporters under control of the *tv3* spermatocyte-specific β2-tubulin promoter, as described in *Materials and Methods*. Western blotting experiments showed that spermatocyte expression of Cdk1(Y15F) resulted in substantially reduced inhibitory phosphorylation of endogenous Cdk1, demonstrating that the transgene activated Cdk1 as predicted (Supplemental Figure S7).

Examination of *tv3*-Cdk1(WT) fluorescence in live cells showed that the protein was enriched on fusomes in both spermatocytes (Figure 5A) and spermatogonia (unpublished data). This observation suggested that transgenic Cdk1 was able to form a complex with fusome-localized Cyclin A (Lilly *et al.*, 2000; Mathieu *et al.*, 2013) This fusome localization of Cdk1(WT)-GFP disappeared when the transgene was expressed in *myt1* mutant spermatocytes, as did endogenous Cyclin A detected by immunolabeling (Supplemental Figure S8). When *tv3*-driven Cdk1(Y15F) was expressed in otherwise wild-type spermatocytes, we observed obvious fusome defects in stage S5–S6 spermatocytes (Figure 5B). This phenotype was less extreme than the fusome defect of *myt1* mutant spermatocytes (compare Figures 2A and 5B), possibly due to limitations in endogenous cyclins needed for complexes with Cdk1(Y15F).

Endogenous Cdk1 moves into the nucleus at the G2/M transition, exhibiting dynamics linked with M-phase progression (Gonczy *et al.*, 1994; Gavet and Pines, 2010). At the stage when fusomes normally disassemble at the late prometaphase I (red, Figure 5A, arrow) we observed Cdk1(WT) in the nucleus (green, arrowhead, Figure 5A), demonstrating that our reporter recapitulates normal Cdk1 dynamics. The Cdk1(Y15F) reporter also translocated into the nucleus at prometaphase I (Figure 5B, arrowhead), apparently unaffected by fusome defects caused by expression of this transgene.

Next we examined how centrosomes and meiotic spindles were affected by expression of Cdk1(WT) and Cdk1(Y15F) by immunolabeling spermatocytes with antibodies against β–tubulin and AurA-T288p. Spermatocytes expressing Cdk1(WT) had normal bipolar meiotic spindles with engaged centrioles (Figure 5C). In contrast, Cdk1(Y15F) expression resulted in spermatocytes with multipolar meiotic spindles (Figure 5C) and partial male sterility (Table 1). Unlike *myt1* mutants, Cdk1(Y15F)-expressing spermatocytes often had more than four AurA-T288p–labeled foci, suggesting that this transgene might also induce centriole rereplication, which normally occurs during S phase. Western blotting data shown in Supplemental Figure S7 also indicate that inhibitory phosphorylation of endogenous Cdk1 was more affected by expression of Cdk1(Y15F) than by loss of Myt1 activity. These biochemical differences in the regulation of endogenous Cdk1 activity may explain how Cdk1(Y15F) expression could affect centriole replication (Bettencourt-Dias *et al.*, 2005; Habedanck *et al.*, 2005; Tsou and Stearns, 2006). These results show that Cdk1(Y15F) expression recapitulating key features of the *myt1* mutant phenotype is consistent with Myt1 inhibitory phosphorylation of Cdk1 being essential during premeiotic G2-phase arrest.

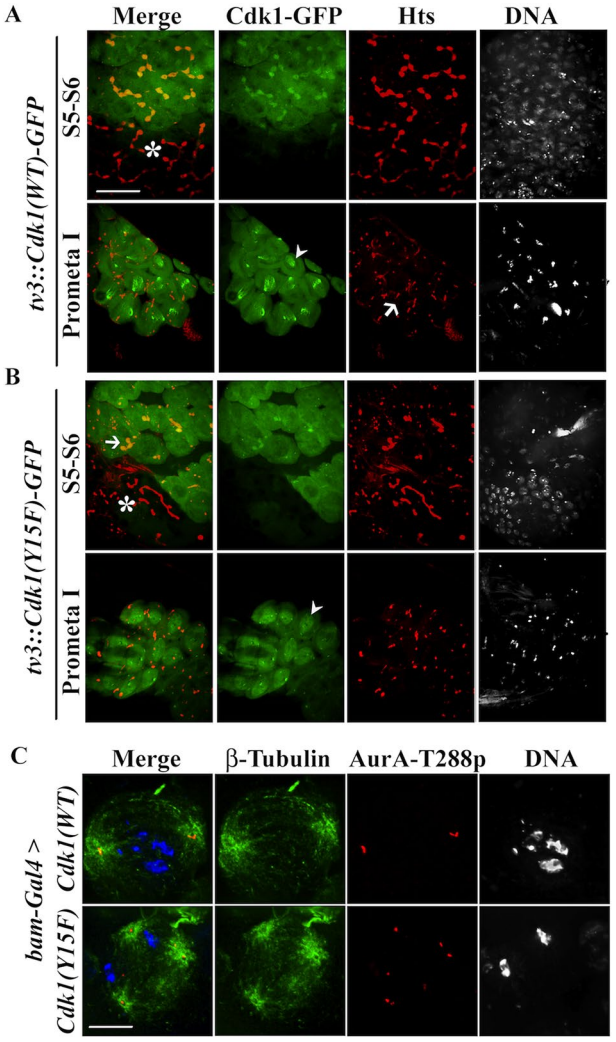

FIGURE 5: Cdk1(WT)-GFP localizes to fusomes, and Cdk1(Y15F) induces *myt1* mutant phenotypes. (A) Fixed stage S5–S6 spermatocytes expressing *tv3:Cdk1(WT)-GFP* were colabeled for Hts (fusomes, red) and DNA. Note that early 16-cell spermatocytes (asterisks) showed no detectable GFP signal. The Cdk1(WT)-GFP signal (green) is primarily cytoplasmic and enriched at fusomes. During prometaphase of meiosis I, Cdk1(WT)-GFP translocates into the nucleus (arrowhead), and the fusomes appeared disassembled (arrow). (B) Expression of *tv3:Cdk1(Y15F)-GFP* appears to trigger fusome disassembly in stages S5–S6 spermatocytes. Note that early-stage spermatocytes (asterisks), where Cdk1(Y15F)-GFP is not expressed, have normal fusomes. Although premeiotic fusome structure is disrupted, nuclear translocation of Cdk1(Y15F)-GFP can be detected in prometaphase I (arrowhead). Scale bar, 16 μm (C) Meiosis I spermatocytes immunolabeled for β-tubulin (green), AuroraA-T288p (red), and DNA (blue). When *Cdk1(WT)-GFP* was expressed, we observed bipolar spindles; however, Cdk1(Y15F)-GFP expression resulted in cells with multipolar meiotic spindles and abnormal numbers of AuroraA-T288p foci. Note that the methanol fixation conditions (see *Materials and Methods*) used to detect microtubules in these experiments quenched the fluorescence signals of the transgenic GFP-tagged Cdk1. Scale bar, 10 μm.

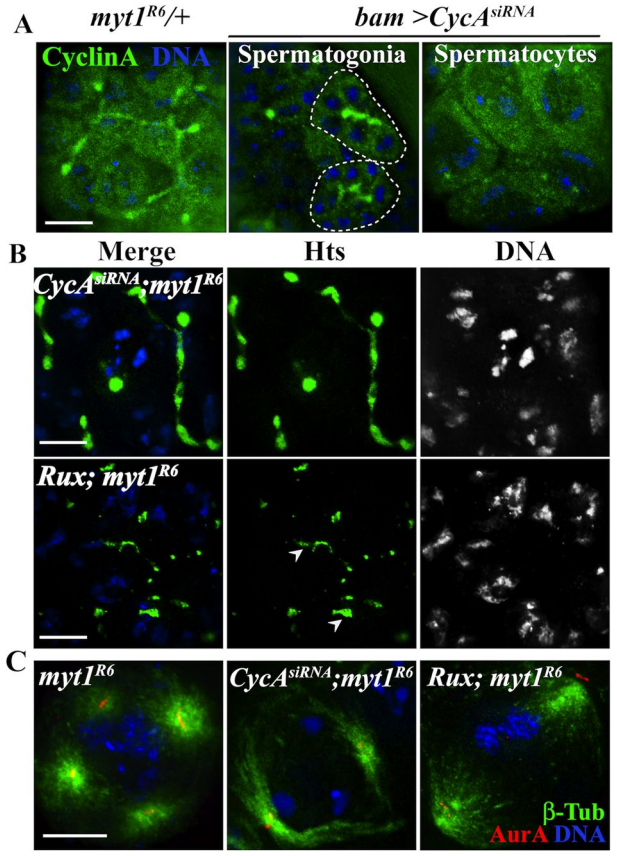

FIGURE 6: Down-regulation of CyclinA/Cdk1 activity suppresses *myt1* mutant premeiotic organelle defects. (A) Control spermatocytes immunolabeled for Cyclin A (green) and DNA (blue) showing diffuse cytoplasmic labeling and fusome-localized signal. RNAi by *bam-Gal4* > $CycA^{siRNA}$ did not affect Cyclin A fusome enrichment in spermatogonia (circled) or diffuse cytoplasmic labeling, but fusome localization in the spermatocytes was undetectable. (B) *myt1* mutant spermatocytes labeled for Hts (green) and DNA (blue). Depletion of Cyclin A by *bam-Gal4* > $CycA^{siRNA}$ restored Hts-labeled fusomes in *myt1* mutants (75%; 57 cysts). Expression of *UASp-Rux* in *myt1* mutants resulted in a partial restoration (82%; 50 cysts) of fusomes. (C) Meiosis I meiotic spindles immunolabeled for β-tubulin (green), AuroraA-T288p (red), and DNA (blue), showing that *bam* > $CycA^{siRNA}$ (87%, $n = 186$) or *bam*>*UASp-Rux* (96%, $n = 129$) expression could rescue the *myt1*-mutant spindle defect. Scale bar, 10 μm.

Myt1 regulation of Cyclin A/Cdk1 prevents premeiotic cytoplasmic organelle defects

Because Cyclin A is expressed throughout premeiotic G2 phase (Lilly *et al.*, 2000), the essential meiotic function of Myt1 might be to regulate Cyclin A/Cdk1. To test this idea, we examined whether depletion of endogenous Cyclin A by RNAi would suppress defects associated with loss of Myt1 activity. As a control for this experiment, we examined the effects of *bam*-driven $CycA^{siRNA}$ by Western blotting testes extracts and probing for Cyclin A (Lehner and O'Farrell, 1990). We detected two bands: a 56-kDa protein, which was markedly reduced in the $CycA^{siRNA}$ sample, and a 70-kDa protein, which was not affected (Supplemental Figure S9A). Cyclin A corresponding to the expected 56-kDa band was therefore effectively depleted under the conditions of our experiment. Fusome localization of endogenous Cyclin A was not detectable by immunolabeling in these *bam*-driven $CycA^{siRNA}$ spermatocytes, unlike the *myt1/+* controls (Figure 6A), confirming that Cyclin A was effectively depleted. When we examined spermatocytes expressing $CycA^{siRNA}$ in a *myt1* mutant background, we observed that the *myt1* fusome defect was suppressed (compare Figure 2, A and C, with Figure 6B). To quantify this effect, we counted cysts with intact fusomes at stages S1–S6. In spermatocytes expressing *bam*-driven $CycA^{siRNA}$ in a *myt1* background, 75% of the cysts analyzed had intact fusomes, 21% were partially intact, and 4% were disrupted ($n = 57$), indicating that depletion of Cyclin A rescued the *myt1* mutant fusome defect. *bam*-driven $CycA^{siRNA}$ expression also rescued the multipolar meiotic spindle defect of the *myt1* mutants (Figure 6C). To quantify this rescue, we counted disengaged centrioles in stage S5–to–prometaphase I spermatocytes and observed that only 13% of *myt1* mutant cells analyzed ($n = 186$) showed premature centriole disengagement when Cyclin A was depleted (vs. 92% without rescue; Figure 4C). These results indicate that *myt1* centriole defects were due to misregulation of Cyclin A/Cdk1 activity.

Although the controls for *bam*-driven $CycA^{siRNA}$ showed no effect on the phenotype during premeiotic G2 phase or early stages of meiosis I, these spermatocytes only progressed as far as metaphase–anaphase I before differentiating into 16-cell onion-stage spermatids (Supplemental Figure S9B). Cyclin A is therefore required for progression through meiosis I. In contrast, parallel experiments to examine the effect of Cyclin B depletion by expression of $CycB^{siRNA}$ with *bam-Gal4* (Supplemental Figure S10A) or *topi*-Gal4 (unpublished data) showed no detectable effects on the phenotype, and Cyclin B levels appeared similar on Western blots comparing control and *myt1* mutants expressing $CycB^{siRNA}$ (Supplemental Figure S10B). Because endogenous Cyclin B is normally expressed very late in G2 phase, we conclude from these results that there was likely insufficient time for RNAi to have any effect.

We also manipulated expression of Roughex (Rux), a Cyclin A–specific Cdk inhibitor (Thomas *et al.*, 1994; Foley *et al.*, 1999) that physically interacts with Cyclin A/Cdk1 during male meiosis (Gonczy *et al.*, 1994). Examination of rux^{8} mutants and spermatocytes ectopically expressing *Rux* with *bam-Gal4* as controls showed normal Hts-labeled fusomes (Supplemental Figure S11), which we quantified by counting cysts with intact fusomes. Expression of *bam*-driven *Rux* in a *myt1/+* control background had no effect, with 100% cysts with normal fusomes (24 cysts). When Rux was expressed in a *myt1* mutant, we observed a partial rescue of the fusome defect (Figure 6B; 12% of cysts with normal, 82% with partial, and 6% with abnormal fusomes; $n = 50$ cysts). *bam*-driven *Rux* expression also almost completely rescued *myt1*-mutant premature centriole disengagement, as quantified in stage S5–to–prometaphase I spermatocytes (only 4% disengaged; $n = 129$). The *bam*-driven *Rux* expression also rescued *myt1*-mutant meiotic spindle defects (Figure 6C) and partially suppressed male sterility (Table 1). We therefore concluded from all of these results that Myt1 inhibition of Cyclin A/Cdk1 is essential for both fusome integrity and normal centrosome behavior during *Drosophila* male meiosis.

DISCUSSION

Prolonged cell cycle arrest in premeiotic G2 phase is a characteristic feature of meiosis. In this study of *Drosophila* male meiosis, we investigated functions of the Cdk1 inhibitory kinase Myt1 that are essential for male fertility. We discovered that loss of Myt1 activity caused disruption of intercellular bridges (fusomes) and premature centriole disengagement during premeiotic G2 phase, resulting in *myt1* spermatocytes entering meiosis I with multipolar meiotic spindles. Myt1 protects fusome integrity and promotes normal centrosome behavior by a novel mechanism involving regulation of Cyclin A/Cdk1.

Myt1 is required for integrity of ER-derived intercellular bridges

Previous studies reported that Myt1 inhibitory phosphorylation of Cyclin B/Cdk1 regulates an "organelle-based checkpoint" mechanism in mammalian cells to prevent Golgi ribbon fragmentation during G2 phase and delay the G2/M transition (Sütterlin *et al.*, 2002; Colanzi *et al.*, 2007; Feinstein and Linstedt, 2007; Rabouille and Kondylis, 2007; Villeneuve *et al.*, 2013; Valente and Colanzi, 2015). The Golgi apparatus is organized as independent stacks in *Drosophila* spermatocytes, and these were not affected by loss of Myt1 activity. Instead, we observed that disruption of endomembrane intercellular bridges called fusomes was the earliest meiotic defect observed in G2 phase–arrested premeiotic *myt1* mutant spermatocytes, several days before these cells actually divide. Fusomes are endomembrane-derived stable intercellular bridges connecting germline cells that undergo developmental remodeling at the mitotic–meiotic transition precisely when loss of Myt1 first noticeably affects the phenotype (Hime *et al.*, 1996; Lighthouse *et al.*, 2008; Eikenes *et al.*, 2013). We therefore identified a new Myt1 mechanism required for normal behavior of a germline-specific endomembrane organelle during early meiosis of *Drosophila* spermatogenesis.

The fusome defects observed in *myt1* mutants can be suppressed by depletion of Cyclin A or ectopic Wee1 and phenocopied by a transgenic Cdk1 variant that is refractory to inhibitory phosphorylation. These findings all support our conclusion that the essential meiotic function of Myt1 is to inhibit Cyclin A/Cdk1 activity. Loss of this novel Myt1 mechanism and disruption of fusome integrity did not result in a premature G2/MI transition, however, so this mechanism does not fulfill the classical definition of a cell cycle checkpoint (Hartwell and Weinert, 1989).

Loss of Myt1 causes premature Polo-mediated meiotic centriole disengagement

Phenotypic analysis of *myt1* mutants also revealed that Myt1 activity prevents premature centriole disengagement during premeiotic G2-phase arrest. Spermatocytes lacking Myt1 activity therefore initiated meiotic cell divisions with multipolar spindles, a defect expected to cause aneuploidy and contribute to male sterility. This defect was suppressed by spermatocyte-specific depletion of the mitotic Polo kinase, which regulates centrosome dynamics, including centriole disengagement during spermatogenesis (Herrmann *et al.*, 1998; Riparbelli *et al.*, 2014), in addition to SAK (Plk4) regulating centriole replication (Stevens *et al.*, 2010; Dzhindzhev *et al.*, 2014).

In mammalian cells, Polo-related (Plk1) kinases regulate centriole disengagement by several mechanisms involving anaphase-promoting complex/cyclosome–mediated degradation of Sas6 (Strnad *et al.*, 2007; Zitouni *et al.*, 2014), securin (Tsou *et al.*, 2009; Hatano and Sluder, 2012; Lee and Rhee, 2012), cohesin (Schöckel *et al.*, 2011; Oliveira and Nasmyth, 2013), and the linker protein Cep68 (Pagan *et al.*, 2015). Large, genetically tractable *Drosophila* spermatocytes therefore offer an attractive new experimental platform for investigating how Polo-mediated centriole disengagement mechanisms are influenced by Myt1 regulation of Cyclin A/Cdk1.

Regulation of Cyclin A/Cdk1 during *Drosophila* male meiosis

Cyclin A is the only essential mitotic cyclin in *Drosophila* (Jacobs *et al.*, 1998). It has been difficult to assign specific functions to Cyclin A because of its partial redundancy with Cyclins B and B3 during development (Reber *et al.*, 2006; McCleland and O'Farrell, 2008; Yuan *et al.*, 2012b). Here we found that spermatocytes depleted for Cyclin A arrest in metaphase of meiosis I with condensed chromatin and mature, separated centrosomes, demonstrating that Cyclin A is specifically required during male meiosis I. Similar phenotypes were described for temperature-sensitive *Cdk1* mutants (Sigrist *et al.*, 1995) and *Cdc25*^{twe} mutants lacking the meiotic phosphatase that removes inhibitory phosphates from Cyclin B/Cdk1 (Alphey *et al.*, 1992; Courtot *et al.*, 1992), indicating that meiotic Cyclin A/Cdk1 activation also depends on Cdc25^{twe}.

Cyclin A localizes to fusomes during male germline development (Lilly *et al.*, 2000). This behavior is required for a spindle orientation checkpoint operating during germline mitotic stem cell divisions (Yuan *et al.*, 2012a); however, the functional significance of Cyclin A fusome localization during meiosis was unclear. We propose the following model to explain how Myt1 regulation of Cyclin A/Cdk1 is used to coordinate male meiosis (Figure 7). During premeiotic G2 phase, Cyclin A is synthesized and sequestered in fusomes as a phosphoinhibited Cyclin A/Cdk1 complex (Figure 7A). In late G2 phase, developmentally regulated synthesis of Cyclin B and Cdc25^{twe} produces active Cyclin B/Cdk1, triggering inhibition of Myt1 and fusome disassembly to release the sequestered Cyclin A/Cdk1 (Figure 7B). Myt1-mediated inhibitory phosphorylation

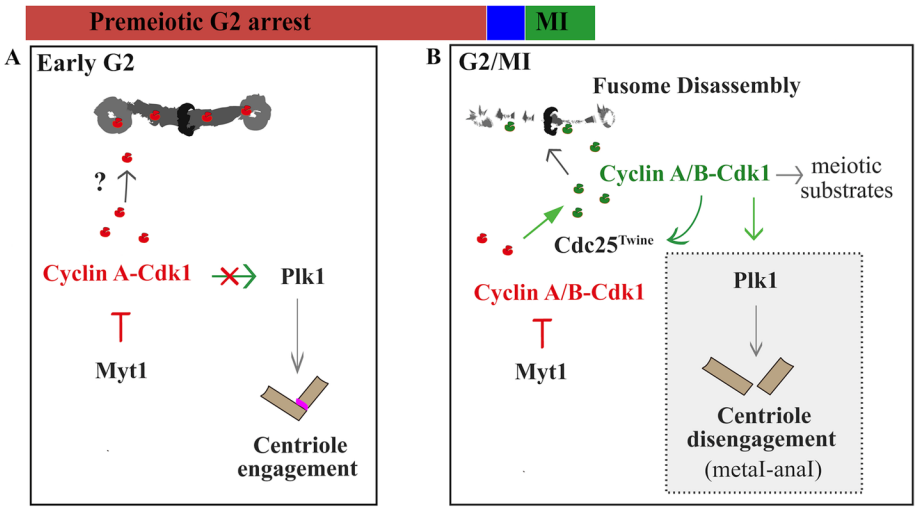

FIGURE 7: Two-step regulation of Cdk1 activity during *Drosophila* male meiosis. The model describes a sequential mechanism for regulation of Cdk1 activity during *Drosophila* male meiosis. (A) As spermatocytes grow during premeiotic G2-phase arrest, Cyclin A/Cdk1 complexes accumulate, but fusomes and centrosomes are protected from premature Cdk1 activity by Myt1-mediated inhibitory phosphorylation. (B) Cdc25^{Twe}-dependent activation of Cyclin A/Cdk1 and newly synthesized Cyclin B/Cdk1 at prometaphase I catalyzes phosphorylation of multiple mitotic targets, driving fusome disassembly and Polo-mediated centriole disengagement in late meiosis I. This model depicts fusomes functioning as a platform for sequestering inhibited Cyclin A/Cdk1 (and other cell cycle regulators) until Cdc25^{Twe}-dependent Cdk1 activation in mature spermatocytes triggers fusome disassembly at G2/MI. In the *myt1* mutants, failure to inhibit Cyclin A/Cdk1 results in premature fusome disassembly and centriole disengagement, showing that these processes can be uncoupled from other aspects of meiotic progression that are regulated by Cdc25^{Twe}-dependent Cdk1 activation.

of Cyclin A/Cdk1 therefore plays a dual role during *Drosophila* male meiosis, preventing both destabilization of fusomes and premature activation of Polo-mediated centriole disengagement mechanisms. Looked at from this perspective, Myt1 inhibition of Cyclin A/Cdk1 coordinates cytoplasmic organelle remodeling with meiotic processes that are regulated by Cyclin B/Cdk1 activity during the G2/MI transition.

Studies of oocyte maturation in other experimental systems focused on how Myt1 inhibition of Cyclin B/Cdk1 restricts positive feedback mechanisms that drive "all-or-none" G2/MI transitions (Ruiz *et al.*, 2010; Gaffre *et al.*, 2011; Santos *et al.*, 2012). In our system, the existence of developmental mechanisms that delay Cyclin B synthesis until late premeiotic G2 phase allowed us to discover that regulation of Cyclin A/Cdk1 activity is crucial for normal endomembrane and centrosome dynamics. Cyclin A/Cdk1 activity also regulates mitotic ER reorganization during the rapid syncytial cycles of early *Drosophila* embryonic development (Bergman *et al.*, 2015). Insights gained from studying the role of Myt1 during *Drosophila* male meiosis may therefore be relevant to investigators studying cell cycle regulatory mechanisms that are used to coordinate Cyclin A and Cyclin B/Cdk1 activities in other developmental contexts.

MATERIALS AND METHODS

Generation of Myt1 transgenic reporter lines

D. melanogaster cDNA encoding dMyt1 was amplified with primers dMyt forward, CACCATGGAAAAGCATCATCG, and dMyt reverse, TCACTCGTCGTCATATTCCAGGA. Amplified DNA was subcloned into a pENTR vector by TOPO cloning (Invitrogen, Carlsbad, CA) and moved into destination vectors via Gateway recombineering. EGFP-tagged Myt1 was cloned into the UASp vector (Brand and Perrimon, 1993) for Gal4-inducible germline expression. We also made constructs directly controlled by a testes-specific β2-tubulin (*tv3*) promoter for expression in mid- to late-stage spermatocytes (Wong *et al.*, 2005). Similar procedures were used to subclone Cdk1(WT), Cdk1(T14A), Cdk1Y15F), and Cdk1(T14A, Y15F) alleles into the β2-tubulin (*tv3*)-driven, GFP-tagged vector (a gift from J. Brill, University of Toronto, Canada) and to construct UASp-Wee1;VFP (details available on request). Transgenic strains were generated by P-element–mediated transformation (BestGene, Chino Hills, CA). The UASp-Myt1 reporter was tested for complementation of *myt1*-mutant bristle defects (Jin *et al.*, 2008) by expressing EGFP-Myt1 in the sensory organ lineage with *neuralized Gal-4* (Yeh *et al.*, 2000). This fully rescued the *myt1* bristle phenotype (100% normal bristles; unpublished data), confirming that EGFP-Myt1 was functional in vivo.

Fly stocks

Transgenic *bam-Gal4* (McKearin and Spradling, 1990; Chen and McKearin, 2003) and *topi-Gal4* (Raychaudhuri *et al.*, 2012) were used to express transgenic proteins in late spermatogonia/early spermatocytes and mature spermatocytes, respectively. Mutant fly strains were recombinant homozygous viable $myt1^{1}$ ($myt1^{R6}$ labeling in the figures designates the recombinant line carrying $myt1^{1}$ that is described in Jin *et al.*, 2008), rux^{8} (Thomas *et al.*, 1994), recombinant, homozygous viable wee^{ES1} (Price *et al.*, 2000), and $twine^{1}$ (Alphey *et al.*, 1992; Courtot *et al.*, 1992). Transgenic reporters obtained from other researchers were *UASp::EGFP-KDEL* (Snapp *et al.*, 2004), *UASp::Rux* (Gonczy *et al.*, 1994), $UASp::CyclinA^{TRiP}$ (Harvard Medical School, Boston MA; *P*(TRiP.GLV21059)), $UASp\text{-}CyclinA^{siRNA}$ (Vienna *Drosophila* Resource Center [VDRC] ID 103595), $UASp\text{-}CyclinB^{siRNA}$ (VDRC ID 109611), and $UASp\text{-}Polo^{siRNA}$ (VDRC ID 20177).

Immunocytochemistry

Testes were dissected from 1- to 2-d-old adult males and immediately transferred into a drop of phosphate-buffered saline (PBS) on a coverslip. The tip of the testes was carefully teased apart, and a polylysine-coated glass slide was used to gently squash out the spermatocytes. Slides were then frozen with liquid nitrogen to remove the coverslip and stored in 95% ethanol. Frozen squashes were fixed in 4% paraformaldehyde (PFA) at room temperature for 7–10 min and then permeabilized in a drop of 0.3% Triton X-100 and 0.3% sodium deoxycholate in PBS for 10 min. After a brief wash with a drop of PBT (0.1% Triton X-100 in PBS), the slides were incubated in 5% bovine serum albumin (BSA)–PBT blocking buffer for 1 h before incubation in the appropriate dilution of primary antibodies overnight at 4°C. To visualize microtubules and centrosomes, testes squashes were prefixed in 100% methanol for 5 min before transfer to cold acetone for 1–2 min and then incubated in PBS with 0.5% acetic acid and 1% Triton X-100 for 10 min. The slides were then briefly washed with PBT and blocked in 5% blocking buffer for 1 h. These fixation conditions quenched the fluorescence of the transgenic fusion proteins (no GFP in Figures 4A and 5C and Supplemental Figures S5 and S6, B and C). The following primary antibodies and concentrations were used for immunolabeling: mouse anti-BrdU (clone G3G4; Developmental Studies Hybridoma Bank [DSHB], Iowa City, IA; used at 1:20), rabbit anti–Lava lamp (Sisson *et al.*, 2000; a gift from O. Papoulas, University of Texas at Austin; used at 1:100), guinea pig anti-Sa (Chen *et al.*, 2005; a gift from M. T. Fuller, Stanford University; 1:500), mouse anti-Hts (Yue *et al.*, 1992; Zaccai and Lipshitz, 1996; DSHB clone 1B1; 1:5), mouse anti–α-spectrin (Dubreuil *et al.*, 1987; clone 3A9; DSHB; 1:500), rabbit anti-anillin (Field and Alberts, 1995; a gift from C. Field, Harvard University; 1:300), mouse anti–GTU-88 (T6557; Sigma-Aldrich, St. Louis, MO; 1:100), rabbit anti–Aurora A-T228P (3091; Cell Signaling; 1:500), and mouse anti–Cyclin A (Lehner and O'Farrell, 1989; clone A12; DSHB; 1:10). After primary antibody labeling overnight, the slides were washed and incubated with fluorescent secondary antibodies (Alexa 488 or Alexa 568; Molecular Probes, Eugene, OR) at 1:1000 dilution. DNA was labeled using 8.3 μg/ml Hoechst 33342. Images were acquired with a Zeiss Axioplan microscope equipped with a Retiga EXi charge-coupled device (CCD) camera, and *Z*-stack images were deconvolved and processed using Volocity software.

BrdU pulse-chase assay

One-day-old males were collected and starved for 4–8 h and then fed with 10 mM BrdU (Invitrogen) diluted in 10% grape juice for a 15-min pulse. Flies with pink abdomens were then transferred to fresh vials with normal medium and incubated subsequently at 25°C. At defined intervals after the BrdU pulse, pairs of testes were dissected from 10 males and squashed in PBS, snap frozen with liquid nitrogen, and stored in 95% ethanol. The slides were then fixed in 4% PFA and processed for immunofluorescence as described earlier. To detect the incorporated BrdU, the testes squashes were treated with 2.2 N HCl for 2 min and 2 M Borax for 10 min, followed by a brief wash in PBT. Testes squashes were then blocked in PBT and incubated with mouse anti-BrdU antibodies overnight.

Western blot analysis

From 8 to 20 testes (depending on the antibodies used) were dissected in PBS supplemented with 2 mM sodium orthovanadate and 10 mM sodium fluoride and then stored at −20°C until ready to use. The testes were subsequently lysed with SDS–PAGE sample buffer and boiled for 7–10 min before being loaded onto polyacrylamide gels. Protein extracts were separated on 10% SDS–PAGE gels,

transferred to Hybond P membrane (Amersham), and then blocked in 5% BSA plus TBST (10 mM Tris-HCl, 150 mM NaCl, and 0.2% Tween-20) before incubation with primary antibodies overnight at 4°C. Phosphospecific Cdk1 antibodies (Cell Signaling) were used at the following concentrations: rabbit anti-Cdk1-T14p (2543), 1:1000, and rabbit anti-Cdk1-Y15p (9111), 1:5000. Mouse anti-GFP (Clontech; 1:5000) was used to label EGFP-Myt1 on Western blots. The labeled proteins were detected using anti-rabbit or anti-mouse secondary antibodies conjugated to horseradish peroxidase (Amersham), and the blots were developed using an ECL Plus/Prime Kit (GE Healthcare).

Male sterility assays

From 20 to 30 individual males were analyzed for each genotype shown in Table 1. Single 1- to 2-d-old males were each crossed with three young *yw* virgin females and the total number of adult progeny from the first brood counted as a measure of male fertility (Gonczy *et al*., 1994). We used *myt1*^{R6}*/+* heterozygous males as positive (fertile) controls.

Transmission electron microscopy

Lacramioara Fabian (University of Toronto, Canada) kindly helped us prepare testes samples for transmission electron microscopy using a method adapted from Tokuyasu *et al*. (1972). Testes were dissected in cold glutaraldehyde (2% in 0.1 M phosphate buffer, pH 7.4), fixed for 2 h at 4°C, rinsed three times with cold PBS, and postfixed at 4°C for 2 h in 2% osmium tetroxide (diluted in PBS) before dehydration in ethanol (5, 10, 20, and 50%) and equilibration at room temperature in 100% ethanol. The testes samples were embedded in propylene oxide and left in Epon 812 overnight at 60°C under vacuum. Thin (70–150 nm) sections were cut using a 65 (Reichert UltraCut E) ultramicrotome and stained with 2% uranyl acetate and lead citrate for imaging with a Philips/FEI (Morgagni) transmission electron microscope equipped with a Gatan (CCD) camera.

ACKNOWLEDGMENTS

We gratefully acknowledge Lacramioara (Lala) Fabian and Julie Brill for assistance with transmission electron microscopy sample preparation, Arlene Oatway (Microscopy Facility, University of Alberta, Edmonton, Canada), and the Molecular Biology Service Unit, University of Alberta. Ross Fitzimmons constructed the UASp-Weee1:VFP construct, and Erica Zhou, Madhur Parashar, and Eliza D'Souza helped with the male sterility assays. We thank for advice Martin Srayko, Sarah Hughes, Gordon Chan, Maryam Ataiem, Guy Tanentzapf, Margaret Fuller, Steve DiNardo, Alan Spradling, Timothy Megraw, and Jordan Raff. Antibodies or fly strains were generously supplied by Christian Lehner, Margaret Fuller, Julie Brill, Jordan Raff, Steve DiNardo, Andrew Swan, Timothy Megraw, the Developmental Studies Hybridoma Bank (University of Iowa), the Bloomington *Drosophila* Center, the Vienna *Drosophila* Resource Center, and the TRiP collection at Harvard Medical School (supported by National Institutes of Health/National Institute of General Medical Sciences Grant R01-GM084947). Funding for this research was provided by the Natural Sciences and Engineering Research Council of Canada.

REFERENCES

Alphey L, Jimenez J, White-Cooper H, Dawson I, Nurse P, Glover DM (1992). twine, a cdc25 homolog that functions in the male and female germline of Drosophila. Cell 69, 977–988.

Ayeni JO, Varadarajan R, Mukherjee O, Stuart DT, Sprenger F, Srayko M, Campbell SD (2014). Dual phosphorylation of cdk1 coordinates cell proliferation with key developmental processes in Drosophila. Genetics 196, 197–210.

Baker CC, Fuller MT (2007). Translational control of meiotic cell cycle progression and spermatid differentiation in male germ cells by a novel eIF4G homolog. Development 134, 2863–2869.

Baker CC, Gim BS, Fuller MT (2015). Cell type-specific translational repression of Cyclin B during meiosis in males. Development 142, 3394–3402.

Belloni G, Sechi S, Riparbelli MG, Fuller MT, Callaini G, Giansanti MG (2012). Mutations in Cog7 affect Golgi structure, meiotic cytokinesis and sperm development during Drosophila spermatogenesis. J Cell Sci 125, 5441–5452.

Bergman ZJ, Mclaurin JD, Eritano AS, Johnson BM, Sims AQ, Riggs B (2015). Spatial reorganization of the endoplasmic reticulum during mitosis relies on mitotic kinase Cyclin A in the early Drosophila embryo. PLoS One 10, e0117859.

Bettencourt-Dias M, Rodrigues-Martins A, Carpenter L, Riparbelli M, Lehmann L, Gatt MK, Carmo N, Balloux F, Callaini G, Glover DM (2005). SAK/PLK4 is required for centriole duplication and flagella development. Curr Biol 15, 2199–2207.

Brand AH, Perrimon N (1993). Targeted gene expression as a means of altering cell fates and generating dominant phenotypes. Development 118, 401–415.

Burrows AE, Sceurman BK, Kosinski ME, Richie CT, Sadler PL, Schumacher JM, Golden A (2006). The C. elegans Myt1 ortholog is required for the proper timing of oocyte maturation. Development 133, 697–709.

Cabral G, Sans SS, Cowan CR, Dammermann A (2013). Multiple mechanisms contribute to centriole separation in C. elegans. Curr Biol 23, 1380–1387.

Cenci G, Bonaccorsi S, Pisano C, Verni F, Gatti M (1994). Chromatin and microtubule organization during premeiotic, meiotic and early postmeiotic stages of Drosophila melanogaster spermatogenesis. J Cell Sci 107, 3521–3534.

Chen D, McKearin DM (2003). A discrete transcriptional silencer in the bam gene determines asymmetric division of the Drosophila germline stem cell. Development 130, 1159–1170.

Chen X, Hiller M, Sancak Y, Fuller MT (2005). Tissue-specific TAFs counteract Polycomb to turn on terminal differentiation. Science 310, 869–872.

Colanzi A, Hidalgo Carcedo C, Persico A, Cericola C, Turacchio G, Bonazzi M, Luini A, Corda D (2007). The Golgi mitotic checkpoint is controlled by BARS-dependent fission of the Golgi ribbon into separate stacks in G2. EMBO J 26, 2465–2476.

Cornwell WD, Kaminski PJ, Jackson JR (2002). Identification of Drosophila Myt1 kinase and its role in Golgi during mitosis. Cell Signal 14, 467–476.

Courtot C, Fankhauser C, Simanis V, Lehner CF (1992). The Drosophila cdc25 homolog twine is required for meiosis. Development 116, 405–416.

de Cuevas M, Lilly MA, Spradling AC (1997). Germline cyst formation in Drosophila. Annu Rev Genet 31, 405–428.

Dubreuil R, Byers TJ, Branton D, Goldstein LS, Kiehart DP (1987). Drosophilia spectrin. I. Characterization of the purified protein. J Cell Biol 105, 2095–2102.

Dzhindzhev NS, Tzolovsky G, Lipinszki Z, Schneider S, Lattao R, Fu J, Debski J, Dadlez M, Glover DM (2014). Plk4 phosphorylates Ana2 to trigger Sas6 recruitment and procentriole formation. Curr Biol 24, 2526–2532.

Eikenes AH, Brech A, Stenmark H, Haglund K (2013). Spatiotemporal control of Cindr at ring canals during incomplete cytokinesis in the Drosophila male germline. Dev Biol 377, 9–20.

Eyers PA, Erikson E, Chen LG, Maller JL (2003). A novel mechanism for activation of the protein kinase Aurora A. Curr Biol 13, 691–697.

Feinstein TN, Linstedt AD (2007). Mitogen-activated protein kinase kinase 1-dependent Golgi unlinking occurs in G2 phase and promotes the G2/M cell cycle transition. Mol Biol Cell 18, 594–604.

Field CM, Alberts BM (1995). Anillin, a contractile ring protein that cycles from the nucleus to the cell cortex. J Cell Biol 131, 165–178.

Foley E, O'Farrell PH, Sprenger F (1999). Rux is a cyclin-dependent kinase inhibitor (CKI) specific for mitotic cyclin-Cdk complexes. Curr Biol 9, 1392–1402.

Franklin-Dumont TM, Chatterjee C, Wasserman SA, Dinardo S (2007). A novel eIF4G homolog, Off-schedule, couples translational control to meiosis and differentiation in Drosophila spermatocytes. Development 134, 2851–2861.

Fuller MT (1998). Genetic control of cell proliferation and differentiation in Drosophila spermatogenesis. Semin Cell Dev Biol 9, 433–444.

Gaffre M, Martoriati A, Belhachemi N, Chambon JP, Houliston E, Jessus C, Karaiskou A (2011). A critical balance between Cyclin B synthesis and Myt1 activity controls meiosis entry in Xenopus oocytes. Development 138, 3735–3744.
Gavet O, Pines J (2010). Progressive activation of CyclinB1-Cdk1 coordinates entry to mitosis. Dev Cell 18, 533–543.
Gonczy P, Thomas BJ, DiNardo S (1994). roughex is a dose-dependent regulator of the second meiotic division during Drosophila spermatogenesis. Cell 77, 1015–1025.
Greenbaum MP, Iwamori T, Buchold GM, Matzuk MM (2011). Germ cell intercellular bridges. Cold Spring Harb Perspect Biol 3, a005850.
Habedanck R, Stierhof YD, Wilkinson CJ, Nigg EA (2005). The Polo kinase Plk4 functions in centriole duplication. Nat Cell Biol 7, 1140–1146.
Hartwell LH, Weinert TA (1989). Checkpoints: controls that ensure the order of cell cycle events. Science 246, 629–634.
Hatano T, Sluder G (2012). The interrelationship between APC/C and Plk1 activities in centriole disengagement. Biol Open 1, 1153–1160.
Herrmann S, Amorim I, Sunkel CE (1998). The POLO kinase is required at multiple stages during spermatogenesis in Drosophila melanogaster. Chromosoma 107, 440–451.
Hime GR, Brill JA, Fuller MT (1996). Assembly of ring canals in the male germ line from structural components of the contractile ring. J Cell Sci 109, 2779–2788.
Inoue D, Sagata N (2005). The Polo-like kinase Plx1 interacts with and inhibits Myt1 after fertilization of Xenopus eggs. EMBO J 24, 1057–1067.
Jacobs HW, Knoblich JA, Lehner CF (1998). Drosophila Cyclin B3 is required for female fertility and is dispensable for mitosis like Cyclin B. Genes Dev 12, 3741–3751.
Jin Z, Homola EM, Goldbach P, Choi Y, Brill JA, Campbell SD (2005). Drosophila Myt1 is a Cdk1 inhibitory kinase that regulates multiple aspects of cell cycle behavior during gametogenesis. Development 132, 4075–4085.
Jin Z, Homola E, Tiong S, Campbell SD (2008). Drosophila myt1 is the major cdk1 inhibitory kinase for wing imaginal disc development. Genetics 180, 2123–2133.
Kao SH, Tseng CY, Wan CL, Su YH, Hsieh CC, Pi H, Hsu HJ (2015). Aging and insulin signaling differentially control normal and tumorous germline stem cells. Aging Cell 14, 25–34.
Karaiskou A, Leprêtre AC, Pahlavan G, Du Pasquier D, Ozon R, Jessus C (2004). Polo-like kinase confers MPF autoamplification competence to growing Xenopus oocytes. Development 131, 1543–1552.
Kishimoto T (2011). A primer on meiotic resumption in starfish oocytes: the proposed signaling pathway triggered by maturation-inducing hormone. Mol Reprod Dev 78, 704–707.
Kornbluth S, Sebastian B, Hunter T, Newport J (1994). Membrane localization of the kinase which phosphorylates p34cdc2 on threonine 14. Mol Biol Cell 5, 273–282.
Lee K, Rhee K (2012). Separase-dependent cleavage of pericentrin B is necessary and sufficient for centriole disengagement during mitosis. Cell Cycle 11, 2476–2485.
Lehner CF, O'Farrell PH (1989). Expression and function of Drosophila cyclin A during embryonic cell cycle progression. Cell 56, 957–968.
Lehner CF, O'Farrell PH (1990). The roles of Drosophila cyclins A and B in mitotic control. Cell 61, 535–547.
Li K, Xu EY, Cecil JK, Turner FR, Megraw TL, Kaufman TC (1998). Drosophila centrosomin protein is required for male meiosis and assembly of the flagellar axoneme. J Cell Biol 141, 455–467.
Lighthouse DV, Buszczak M, Spradling AC (2008). New components of the Drosophila fusome suggest it plays novel roles in signaling and transport. Dev Biol 317, 59–71.
Lilly MA, de Cuevas M, Spradling AC (2000). Cyclin A associates with the fusome during germline cyst formation in the Drosophila ovary. Dev Biol 218, 53–63.
Lin H, Spradling AC (1995). Fusome asymmetry and oocyte determination in Drosophila. Dev Genet 16, 6–12.
Lin H, Yue L, Spradling AC (1994). The Drosophila fusome, a germline-specific organelle, contains membrane skeletal proteins and functions in cyst formation. Development 120, 947–956.
Liu F, Rothblum-Oviatt C, Ryan CE, Piwnica-Worms H (1999). Overproduction of human Myt1 kinase induces a G2 cell cycle delay by interfering with the intracellular trafficking of Cdc2-cyclin B1 complexes. Mol Cell Biol 19, 5113–5123.
Liu F, Stanton JJ, Wu Z, Piwnica-Worms H (1997). The human Myt1 kinase preferentially phosphorylates Cdc2 on threonine 14 and localizes to the endoplasmic reticulum and Golgi complex. Mol Cell Biol 17, 571–583.
Mathieu J, Cauvin C, Moch C, Radford SJ, Sampaio P, Perdigoto CN, Schweisguth F, Bardin AJ, Sunkel CE, McKim K, *et al*. (2013). Aurora B and cyclin B have opposite effects on the timing of cytokinesis abscission in Drosophila germ cells and in vertebrate somatic cells. Dev Cell 26, 250–265.
McCleland ML, O'Farrell PH (2008). RNAi of mitotic cyclins in Drosophila uncouples the nuclear and centrosome cycle. Curr Biol 18, 245–254.
McKearin D (1997). The Drosophila fusome, organelle biogenesis and germ cell differentiation: if you build it. Bioessays 19, 147–152.
McKearin DM, Spradling AC (1990). bag-of-marbles: a Drosophila gene required to initiate both male and female gametogenesis. Genes Dev 4, 2242–2251.
McKim KS, Jang JK, Theurkauf WE, Hawley RS (1993). Mechanical basis of meiotic metaphase arrest. Nature 362, 364–366.
Mueller PR, Coleman TR, Kumagai A, Dunphy WG (1995). Myt1: a membrane-associated inhibitory kinase that phosphorylates Cdc2 on both threonine-14 and tyrosine-15. Science 270, 86–90.
Nakajima H, Yonemura S, Murata M, Nakamura N, Piwnica-Worms H, Nishida E (2008). Myt1 protein kinase is essential for Golgi and ER assembly during mitotic exit. J Cell Biol 181, 89–103.
Nakajo N, Yoshitome S, Iwashita J, Iida M, Uto K, Ueno S, Okamoto K, Sagata N (2000). Absence of Wee1 ensures the meiotic cell cycle in Xenopus oocytes. Genes Dev 14, 328–338.
Oh JS, Han SJ, Conti M (2010). Wee1B, Myt1, and Cdc25 function in distinct compartments of the mouse oocyte to control meiotic resumption. J Cell Biol 188, 199–207.
Oliveira RA, Nasmyth K (2013). Cohesin cleavage is insufficient for centriole disengagement in Drosophila. Curr Biol 23, R601–R603.
Pagan JK, Marzio A, Jones MJ, Saraf A, Jallepalli PV, Florens L, Washburn MP, Pagano M (2015). Degradation of Cep68 and PCNT cleavage mediate Cep215 removal from the PCM to allow centriole separation, disengagement and licensing. Nat Cell Biol 17, 31–43.
Palmer A, Gavin AC, Nebreda AR (1998). A link between MAP kinase and p34(cdc2)/cyclin B during oocyte maturation: p90(rsk) phosphorylates and inactivates the p34(cdc2) inhibitory kinase Myt1. EMBO J 17, 5037–5047.
Price DM, Jin Z, Rabinovitch S, Campbell SD (2002). Ectopic expression of the Drosophila Cdk1 inhibitory kinases, Wee1 and Myt1, interferes with the second mitotic wave and disrupts pattern formation during eye development. Genetics 161, 721–731.
Price D, Rabinovitch S, O'Farrell PH, Campbell SD (2000). Drosophila wee1 has an essential role in the nuclear divisions of early embryogenesis. Genetics 155, 159–166.
Rabouille C, Kondylis V (2007). Golgi ribbon unlinking: an organelle-based G2/M checkpoint. Cell Cycle 6, 2723–2729.
Raychaudhuri N, Dubruille R, Orsi GA, Bagheri HC, Loppin B, Lehner CF (2012). Transgenerational propagation and quantitative maintenance of paternal centromeres depends on Cid/Cenp-A presence in Drosophila sperm. PLoS Biol 10, e1001434.
Reber A, Lehner CF, Jacobs HW (2006). Terminal mitoses require negative regulation of Fzr/Cdh1 by Cyclin A, preventing premature degradation of mitotic cyclins and String/Cdc25. Development 133, 3201–3211.
Riparbelli MG, Gottardo M, Glover DM, Callaini G (2014). Inhibition of Polo kinase by BI2536 affects centriole separation during Drosophila male meiosis. Cell Cycle 13, 2064–2072.
Ruiz EJ, Vilar M, Nebreda AR (2010). A two-step inactivation mechanism of Myt1 ensures CDK1/cyclin B activation and meiosis I entry. Curr Biol 20, 717–723.
Santos SD, Wollman R, Meyer T, Ferrell JE (2012). Spatial positive feedback at the onset of mitosis. Cell 149, 1500–1513.
Schöckel L, Möckel M, Mayer B, Boos D, Stemmann O (2011). Cleavage of cohesin rings coordinates the separation of centrioles and chromatids. Nat Cell Biol 13, 966–972.
Sigrist S, Ried G, Lehner CF (1995). Dmcdc2 kinase is required for both meiotic divisions during Drosophila spermatogenesis and is activated by the Twine/cdc25 phosphatase. Mech Dev 53, 247–260.
Sisson JC, Field C, Ventura R, Royou A, Sullivan W (2000). Lava lamp, a novel peripheral golgi protein, is required for Drosophila melanogaster cellularization. J Cell Biol 151, 905–918.
Snapp EL, Iida T, Frescas D, Lippincott-Schwartz J, Lilly MA (2004). The fusome mediates intercellular endoplasmic reticulum connectivity in Drosophila ovarian cysts. Mol Biol Cell 15, 4512–4521.
Stevens NR, Roque H, Raff JW (2010). DSas-6 and Ana2 coassemble into tubules to promote centriole duplication and engagement. Dev Cell 19, 913–919.

Strnad P, Leidel S, Vinogradova T, Euteneuer U, Khodjakov A, Gonczy P (2007). Regulated HsSAS-6 levels ensure formation of a single procentriole per centriole during the centrosome duplication cycle. Dev Cell 13, 203–213.
Sütterlin C, Hsu P, Mallabiabarrena A, Malhotra V (2002). Fragmentation and dispersal of the pericentriolar Golgi complex is required for entry into mitosis in mammalian cells. Cell 109, 359–369.
Thomas BJ, Gunning DA, Cho J, Zipursky L (1994). Cell cycle progression in the developing Drosophila eye: roughex encodes a novel protein required for the establishment of G1. Cell 77, 1003–1014.
Tokuyasu KT, Peacock WJ, Hardy RW (1972). Dynamics of spermiogenesis in Drosophila melanogaster. I. Individualization process. Z Zellforsch Mikrosk Anat 124, 479–506.
Tsai MY, Wiese C, Cao K, Martin O, Donovan P, Ruderman J, Prigent C, Zheng Y (2003). A Ran signalling pathway mediated by the mitotic kinase Aurora A in spindle assembly. Nat Cell Biol 5, 242–248.
Tsou MF, Stearns T (2006). Mechanism limiting centrosome duplication to once per cell cycle. Nature 442, 947–951.
Tsou MF, Wang WJ, George KA, Uryu K, Stearns T, Jallepalli PV (2009). Polo kinase and separase regulate the mitotic licensing of centriole duplication in human cells. Dev Cell 17, 344–354.
Valente C, Colanzi A (2015). Mechanisms and regulation of the mitotic inheritance of the Golgi complex. Front Cell Dev Biol 3, 79.
Villeneuve J, Scarpa M, Ortega-Bellido M, Malhotra V (2013). MEK1 inactivates Myt1 to regulate Golgi membrane fragmentation and mitotic entry in mammalian cells. EMBO J 32, 72–85.
Vitre BD, Cleveland DW (2012). Centrosomes, chromosome instability (CIN) and aneuploidy. Curr Opin Cell Biol 24, 809–815.
Wang X, Yang Y, Duan Q, Jiang N, Huang Y, Darzynkiewicz Z, Dai W (2008). sSgo1, a major splice variant of Sgo1, functions in centriole cohesion where it is regulated by Plk1. Dev Cell 14, 331–341.
Wells NJ, Watanabe N, Tokusumi T, Jiang W, Verdecia MA, Hunter T (1999). The C-terminal domain of the Cdc2 inhibitory kinase Myt1 interacts with Cdc2 complexes and is required for inhibition of G(2)/M progression. J Cell Sci 112, 3361–3371.
White-Cooper H, Alphey L, Glover DM (1993). The cdc25 homologue twine is required for only some aspects of the entry into meiosis in Drosophila. J Cell Sci 106, 1035–1044.
White-Cooper H, Schafer MA, Alphey LS, Fuller MT (1998). Transcriptional and post-transcriptional control mechanisms coordinate the onset of spermatid differentiation with meiosis I in Drosophila. Development 125, 125–134.
Wilson PG (2005). Centrosome inheritance in the male germ line of Drosophila requires hu-li tai-shao function. Cell Biol Int 29, 360–369.
Wong R, Hadjiyanni I, Wei HC, Polevoy G, McBride R, Sem KP, Brill JA (2005). PIP2 hydrolysis and calcium release are required for cytokinesis in Drosophila spermatocytes. Curr Biol 15, 1401–1406.
Yasuno Y, Kawano J, Inoue YH, Yamamoto MT (2013). Distribution and morphological changes of the Golgi apparatus during Drosophila spermatogenesis. Dev Growth Differ 55, 635–647.
Yeh E, Zhou L, Rudzik N, Boulianne GL (2000). Neuralized functions cell autonomously to regulate Drosophila sense organ development. EMBO J 19, 4827–4837.
Yuan H, Chiang CY, Cheng J, Salzmann V, Yamashita YM (2012a). Regulation of cyclin A localization downstream of Par-1 function is critical for the centrosome orientation checkpoint in Drosophila male germline stem cells. Dev Biol 361, 57–67.
Yuan K, Farrell JA, O'Farrell PH (2012b). Different cyclin types collaborate to reverse the S-phase checkpoint and permit prompt mitosis. J Cell Biol 198, 973–980.
Yue L, Spradling AC, Zaccai M, Lipshitz HD (1992). hu-li tai shao, a gene required for ring canal formation during Drosophila oogenesis, encodes a homolog of adducin. Role of Adducin-like (hu-li tai shao) mRNA and protein localization in regulating cytoskeletal structure and function during Drosophila oogenesis and early embryogenesis. Genes Dev Dev Genet 6, 2443–2454.
Zaccai M, Lipshitz HD (1996). Role of Adducin-like (hu-li tai shao) mRNA and protein localization in regulating cytoskeletal structure and function during Drosophila oogenesis and early embryogenesis. Dev Genet 19, 249–257.
Zitouni S, Nabais C, Jana SC, Guerrero A, Bettencourt-Dias M (2014). Polo-like kinases: structural variations lead to multiple functions. Nat Rev Mol Cell Biol 15, 433–452.